J. Biomed. Eng. Res : 436-442, 2008

MREIT of Postmortem Swine Legs using Carbon-hydrogel Electrodes

Atul S. Minhas, Woo Chul Jeong, Young Tae Kim, Hyung Joong Kim, Tae Hwi Lee and Eung Je Woo

College of Electronics and Information, Kyung Hee University, Korea

(Received October 15, 2008. Accepted December 15, 2008)

Abstract

Magnetic resonance electrical impedance tomography (MREIT) has been suggested to produce cross-sectional conductivity images of an electrically conducting object such as the human body. In most previous studies, recessed electrodes have been used to inject imaging currents into the object. An MRI scanner was used to capture induced magnetic flux density data inside the object and a conductivity image reconstruction algorithm was applied to the data. This paper reports the performance of a thin and flexible carbon-hydrogel electrode that replaces the bulky and rigid recessed electrode in previous studies. The new carbon-hydrogel electrode produces a negligible amount of artifacts in MR and conductivity images and significantly simplifies the experimental procedure. We can fabricate the electrode in different shapes and sizes. Adding a layer of conductive adhesive, we can easily attach the electrode on an irregular surface with an excellent contact. Using a pair of carbon-hydrogel electrodes with a large contact area, we may inject an imaging current with increased amplitude primarily due to a reduced average current density underneath the electrodes. Before we apply the new electrode to a human subject, we evaluated its performance by conducting MREIT imaging experiments of five swine legs. Reconstructed conductivity images of the swine legs show a good contrast among different muscles and bones. We suggest a future study of human experiments using the carbon-hydrogel electrode following the guideline proposed in this paper

Key words : magnetic resonance electrical impedance tomography, magnetic flux density, conductivity image, carbon-hydrogel electrode

Ⅰ. INTRODUCTION

The goal of magnetic resonance electrical impedance tomography (MREIT) is to provide cross-sectional images of a conductivity distribution inside an electrically conducting object with high spatial resolution [1-4]. Woo *et al.* summarized its early progress [5] and Kim *et al.* described the most recent experimental results [6,7]. In MREIT, we inject currents into the imaging object through pairs of surface electrodes. Each imaging current produces a distribution of an induced magnetic flux density. We use an MRI scanner to capture the induced magnetic flux density data inside the object along the direction of the main magnetic field of the scanner. A conductivity image reconstruction algorithm is applied to the data set to produce cross-sectional images of the conductivity distribution.

Corresponding Author : Eung Je Woo
Department of Biomedical Engineering, College of Electronics and Information, Kyung Hee Univ.
1 Seochun, Giheung, Yongin, Gyeonggi, 446-701, Korea
Tel : +82-31-201-2538 / Fax : +82-31-201-2378
E-mail : ejwoo@khu.ac.kr
This work was supported by the SRC/ERC program of MOST/KOSEF (R11-2002-103)

In order to inject current, we need to attach a pair of surface electrodes. A non-magnetic conductor such as the copper can be used in MREIT. If we attach a copper electrode on the surface of the imaging object placed inside the bore of the MRI scanner, it shields the RF signal to produce severe image artifacts in the region near the conductor. In order to avoid this problem, Lee *et al.* and Oh *et al.* suggested a recessed electrode in MREIT [8-11]. The recessed electrode as shown in figure 1(a) is basically an acrylic container (usually in a cylindrical shape) filled with a conductive gel such as agar, animal hide gelatin or TX151 [12]. The gel at the bottom of the container is in contact with the surface of the imaging object and a copper electrode is attached to the gel on the top of the container. An MREIT current source is connected to the copper electrode via a lead wire and imaging current enters the object through the gel. Since the copper is moved away from the object's surface, the RF shielding artifact occurs inside the container around the gel region near the conductor. This makes the image of the object free from the artifact around its peripheral region that makes contact with the recessed electrode.

Though the recessed electrode has been very successful in

phantom and some animal experiments, it has some disadvantages [6,7,10,11]. It is bulky and rigid. We need an electrode holder to attach it on the object's surface. For a good contact of multiple recessed electrodes, we should apply enough holding force to tightly fix them on the surface of the imaging object. This procedure is troublesome and most of all ends up distorting the shape of the object.

To alleviate the problems of the recessed electrode, we suggest a carbon-hydrogel electrode in this paper. We will describe its design for the MREIT imaging experiment of a postmortem swine leg. Verifying its performance from MR and reconstructed conductivity images, we will suggest it for future MREIT imaging study of a human subject. We emphasize that the conductivity imaging of a swine leg itself is our first trial of MREIT imaging of muscles and bones *in situ*. We will discuss a technical problem related with the bone inside the leg. The results of the swine leg imaging experiment using carbon-hydrogel electrodes will be analyzed to derive an experimental procedure for our future *in vivo* human imaging experiments.

II. MATERIALS AND METHODS

A. Design of carbon-hydrogel electrode

The new carbon-hydrogel electrode is shown in figure 1(b). It comprises a custom-designed thin carbon electrode and a layer of hydrogel with conductive adhesive (HUREV Co. Ltd., Korea). The size of the carbon electrode is 80×60×0.0596 mm^3. To verify the effect of RF shielding artifact, two different sizes of 80×60×5.7 mm^3 and 80×60×0.7 mm^3 of hydrogel layer were tested. Conductivity values of the carbon and hydrogel are 2.857×10^4 and 0.17 S/m, respectively. The lead wire attached to the carbon electrode is also made of carbon for better compatibility with an MRI scanner. The resistance of the thick carbon-hydrogel electrode is about 300Ω.

B. Imaging method

We performed MREIT experiments using our 3T MRI scanner (Magnum 3, Medinus Co. Ltd., Korea) with a STR RF coil (130 mm inner diameter, 190 mm outer diameter and 220 mm length) [10]. Placing a swine leg inside the MR scanner with four electrodes attached around it, we injected 10 mA current between a pair of facing electrodes. The Injection Current Non-Linear Encoding (ICNE) pulse sequence, synchronized with current source, with TR/TE=1200/30 ms, was used to scan the swine leg [6,7,13]. The field-of-view (FOV) was 180×180 mm^2, slice thickness was 4 mm, number of slices was 8, number of averaging (NEX) was 8 and image matrix size was 128×128. The pixel size was 1.41×1.41 mm^2. Injecting the first imaging current I_1 between one pair of opposing electrodes, we collected the k-space data from 8 axial slices. The second imaging current I_2 with the same amplitude and duration was injected through the other pair of opposing electrodes to obtain another k-space data. The total scan time was 100 minutes.

C. Imaging experiments for electrode testing

We obtained five swine legs from a local grocery store. Each of them arrived at our laboratory in the morning of the experiment and the elapsed times from butchery were almost same for all the cases. All of them were scanned three times by using three different types of electrodes including previously used recessed electrodes, thin carbon-hydrogel electrodes and thick carbon-hydrogel electrodes and their conductivity images were reconstructed. In each experiment, we placed the swine leg inside the bore of our 3T MRI scanner. We attached four chosen electrodes around the leg. Figure 2(a) shows the thick carbon-hydrogel electrode and (b) is a picture of the swine leg with the four carbon-hydrogel electrodes attached around it. We connected the four electrodes to our custom-designed MREIT current source [14]. By using the imaging

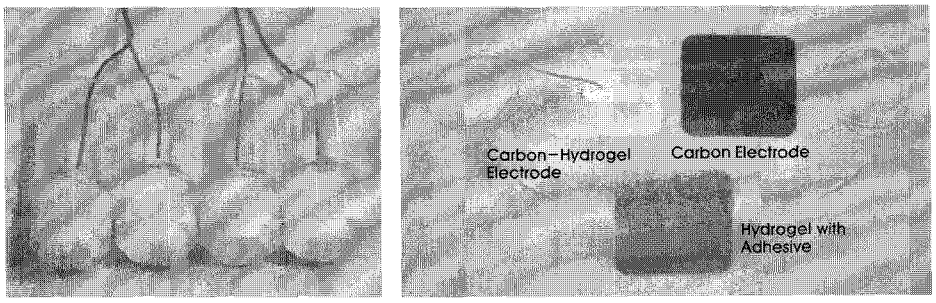

Fig. 1. (a) Recessed electrodes used in previous MREIT experiments. (b) New carbon-hydrogel electrode comprises a thin carbon electrode and a layer of hydrogel with conductive adhesive.

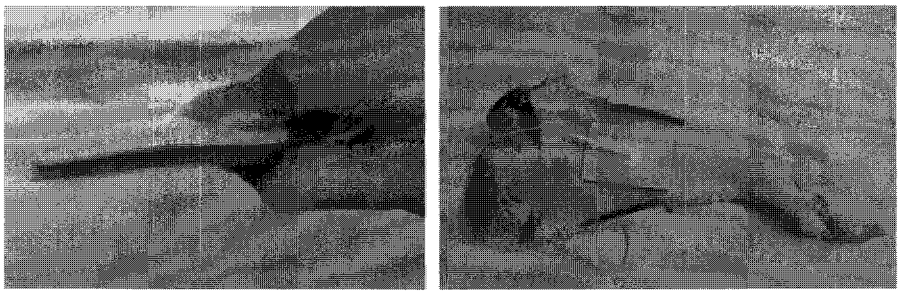

(a) (b)

Fig. 2. (a) Carbon-hydrogel electrode before attachment. (b) A swine leg with four carbon-hydrogel electrodes attached on its leg.

method described in section B, we performed three separate imaging experiments using the three different kinds of electrodes. To compare them, we evaluated the electrode performance indices of induced voltage, boundary shape distortion, artifacts in MR magnitude and B_z images and amount of noise in B_z images.

D. Conductivity image reconstruction

We reconstructed MR magnitude and phase images from the obtained k-space data set. The MR magnitude images were used to build three-dimensional computer models of the swine legs for conductivity image reconstructions. The magnetic flux density images were extracted from the MR phase images. In this paper, we denote the induced magnetic flux densities subject to injection currents I_1 and I_2 as B_{z1} and B_{z2}, respectively. These are z-directional components of induced magnetic flux density vectors where z is the direction of the main magnetic field of the MRI scanner. The amount of noise in a B_z image was evaluated by using the method described in [15]. We performed multi-slice conductivity image reconstructions using the harmonic B_z algorithm [9,16]. Muscle is known to be anisotropic in its conductivity value [17-20]. Due to the limitation of the harmonic B_z algorithm in handling an anisotropic conductivity tensor, we reconstructed equivalent isotropic conductivity images [6].

III. RESULTS

A. Performance of three different types of electrodes

Figure 3 shows MR magnitude images of the first swine leg using three different kinds of four electrodes. From (a), we can see that the recessed electrodes caused severe distortion of the boundary shape. As can be seen in (b) and (c), thin carbon-hydrogel and thick carbon-hydrogel electrodes did not produce any shape distortion. Both copper and carbon electrodes produced RF shielding artifacts, which appeared as dark MR signal in figure 3. The amounts of RF shielding artifacts in (b) and (c) produced by carbon electrodes are considerably smaller than that in (a) from copper electrodes. The thick hydrogel layer in (c) effectively moved the small amount of RF shielding artifact away from the boundary of the imaging object. Figure 4 shows B_z images of the swine leg subject to

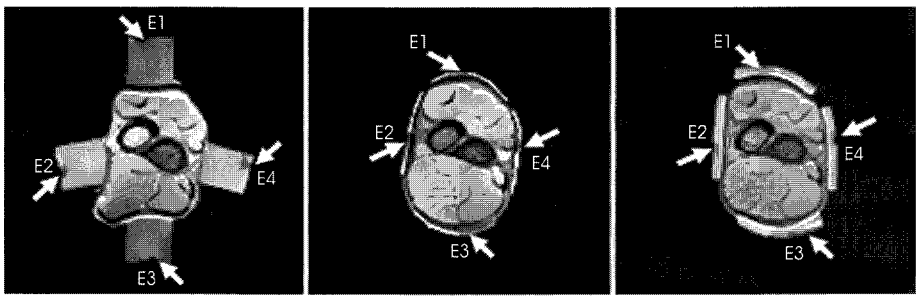

(a) (b) (c)

Fig. 3. MR magnitude images of a swine leg with (a) recessed electrodes, (b) thin carbon-hydrogel electrodes and (c) thick carbon-hydrogel electrodes. E1, E2, E3 and E4 denote four electrodes. White arrows indicate RF shielding artifacts. The amounts of RF shielding artifacts in (b) and (c) produced by carbon electrodes are considerably smaller than that in (a) from copper electrodes.

Table 1. Induced voltages and noise levels with 10 mA current injection.

Electrode	Voltage (E1 and E3) [V]	Voltage (E2 and E4) [V]	Noise in B_z [nT]
Recessed	21.4	19.3	0.72
Thin carbon-hydrogel	16.7	15.7	0.62
Thick carbon-hydrogel	17.1	16.2	0.56

E1, E2, E3 and E4 denote electrodes in figure

the 10 mA current injection between the vertical pair of electrodes. Unlike (a) and (c), we can see that carbon electrodes in (b) produced more artifacts inside the swine leg along the phase encoding direction (the horizontal direction). These artifacts appear as fluctuations in pixel intensities along the horizontal direction as indicated by white arrows.

Table 1 compares induced voltages between two pair of electrodes and amounts of noises in measured B_z images, for the three kinds of electrodes. There are higher voltage drops in recessed electrodes for the same 10 mA current injection compared to both types of carbon-hydrogel electrodes. In terms of the noise level in B_z image, estimated by using the method explained in [15] by Sadleir *et al.*, the thick carbon-hydrogel electrode is the best among three electrode types. From figures 3, 4 and table 1, the overall performance of the thick carbon-hydrogel electrode was superior to the other two types.

B. Reconstructed equivalent isotropic conductivity images

We reconstructed equivalent isotropic conductivity images of the five swine legs from the B_z data sets obtained by using the carbon-hydrogel electrodes. Figure 5 shows typical MREIT images from the third swine leg. MR magnitude and equivalent isotropic conductivity images are shown in (a) and (b), respectively. In (c), we plotted a color-coded image of (b). Figure 6 shows multi-slice images of the third swine leg.

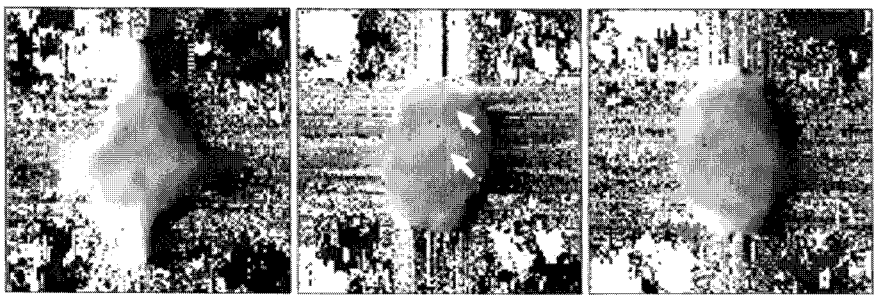

(a) (b) (c)

Fig. 4. B_z images of a swine leg with (a) recessed electrodes, (b) thin carbon-hydrogel electrodes and (c) thick carbon-hydrogel electrodes. Current was injected between the vertical pair of electrodes. Arrows indicate artifacts along the phase encoding direction.

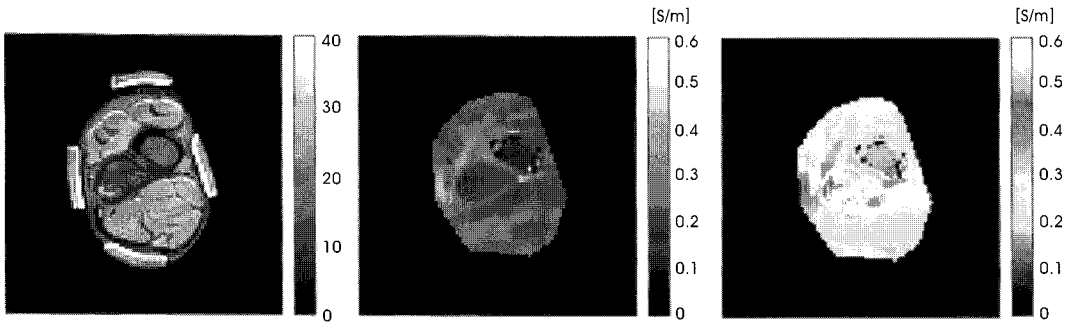

(a) (b) (c)

Fig. 5. Typical MREIT images of a swine leg: (a) MR magnitude image, (b) equivalent isotropic conductivity image and (c) color-coded image of (b).

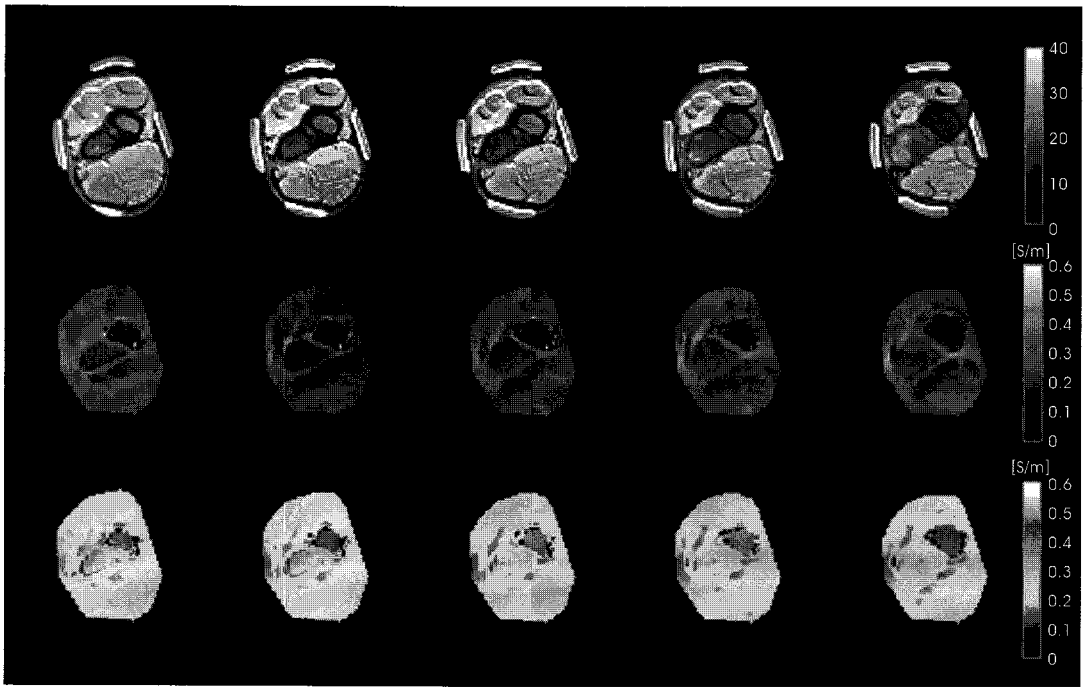

Fig. 6. Multi-slice images of third swine leg. Top, middle and bottom rows are MR magnitude images, equivalent isotropic conductivity images and color-coded conductivity images, respectively.

These images were obtained from six consecutive axial imaging slices. Figure 7 shows the results from the fifth swine leg. Images from the other swine legs were similar though we could observe a clear subject dependency.

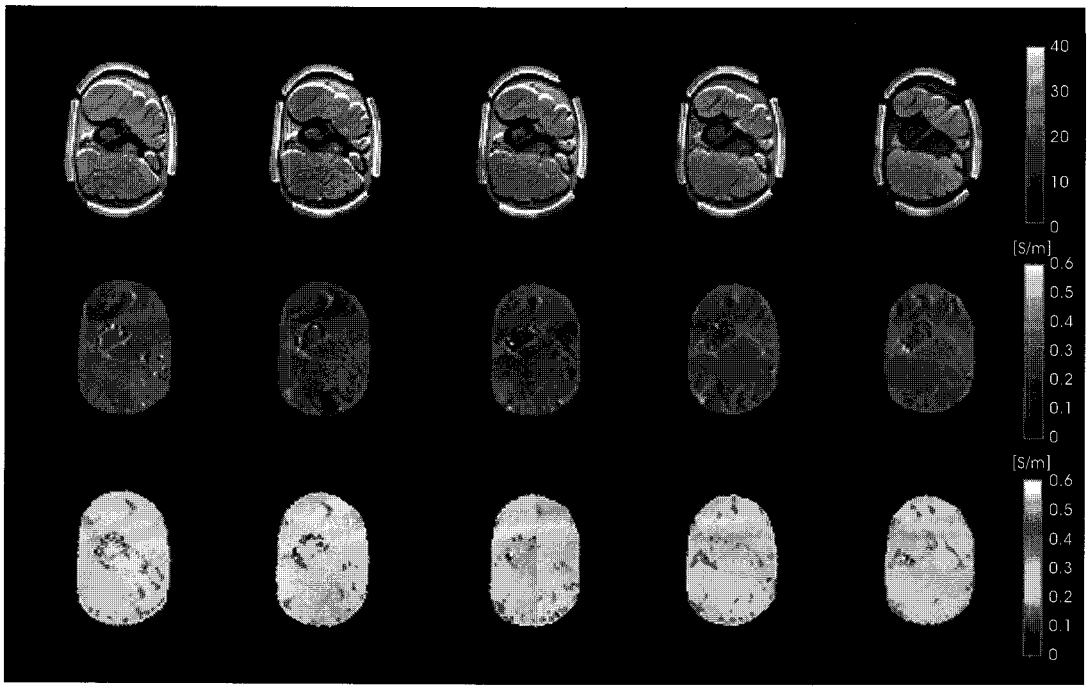

Fig. 7. Multi-slice images of the fifth swine leg. Top, middle and bottom rows are MR magnitude images, equivalent isotropic conductivity images and color-coded conductivity images, respectively.

Ⅳ. DISCUSSION

The recessed electrodes distort the object shape due to higher pressure exerted by the electrode holder while attaching them over the skin. The flexible thin and thick carbon-hydrogel electrodes however, do not need any holder and hence no shape distortion occurs. In order to reduce artifacts in the phase encoding direction, we need to use the thick hydrogel layer to move the conductive carbon away from the skin. Moreover, the thick hydrogel layer is helpful in minimizing the amount of RF shielding artifacts near the boundary of an imaging object. The smaller voltage drop in both the carbon-hydrogel electrodes compared to that of the recessed electrodes is primarily due to their larger surface area. The carbon-hydrogel electrodes with a large contact area produce a smaller current density for given amplitude of an injection current. Therefore, they are advantageous for us to inject current with increased amplitude.

Reconstructed equivalent isotropic conductivity images of the swine legs show a perceivable conductivity contrast among different muscles. Boundary areas of muscles appear to have relatively low conductivity values. Since we reconstructed equivalent isotropic conductivity images, we should be careful in their quantitative interpretation. Further experimental studies of both postmortem and *in vivo* animal subjects are needed to extract physiologically meaningful information from the reconstructed conductivity images. In our future work, we should also adopt numerous animal models that alter conductivity values of tissues inside their legs.

The internal region of the bone including the bone marrow and possibly the sponge bone appear to have relatively low conductivity values. Reconstructed conductivity images show that the outer layer of the bone including the compact bone has low conductivity values though the images are noisy there. These observations qualitatively match well with previous findings on measured conductivity values of extracted bones [17-20]. We would like to postpone further quantitative analysis of reconstructed conductivity values of the bone regions for the following reason.

The dark pixels in an MR magnitude image correspond to a region where its MR signal is weak primarily due to a low proton density. The outer layer of the bone appears to be black in the MR magnitude images due to the MR signal void phenomenon there. This means that the signal-to-noise ratio (SNR) of the MR magnitude image is low in the outer layer of the bone. The magnetic flux density image contains a large amount of noise there since the noise level in an induced magnetic flux density is inversely proportional to the SNR of the MR magnitude image [15,21,22]. This is the main reason why the reconstructed conductivity images show extraneous spurious spikes in the outer layers of the bones. Lee *et al.* observed this phenomenon and suggested an inpainting method to fill-in the problematic region with a synthetic data [23]. Their method requires a careful image segmentation step and this must be incorporated in the image reconstruction algorithm to improve the image quality.

Ⅴ. CONCLUSION AND FUTURE WORK

The flexible carbon-hydrogel electrodes with conductive adhesive significantly simplify the experimental procedure. Their large surface area and good contact with the skin are beneficial for injecting currents in MREIT experiments. The boundary shape distortion is alleviated. A carefully chosen thickness of hydrogel layer significantly reduces the RF shielding artifacts at object boundary and artifacts along the phase encoding direction. We suggest using this new electrode for future imaging study of animal and human subjects.

The high resolution conductivity imaging method in MREIT has reached a stage of routine imaging experiments of postmortem and *in vivo* animals. Accumulating results from numerous animal experiments, we will build an MREIT database. Numerous disease models must be included in the database. Improved image reconstruction algorithms can be validated by using a standard data set in the database. Since there is no other method to compare MREIT conductivity images of living objects *in situ*, we will utilize the conductivity image database to properly interpret a conductivity contrast among tissues.

Based on the results presented in this paper, we propose the following experimental procedure for the future study of our human imaging experiment. In the initial trial of a human experiment, we recommend imaging the lower or upper extremities. First, we apply four carbon-hydrogel electrodes around the human leg, for example. Second, we gradually increase the injection current amplitude from zero mA and record the thresholds of perception and tolerable pain. Third, we determine the amplitude of the imaging current as 90% of the pain threshold, for example. It will be beneficial to use a carbon-hydrogel electrode with a large contact area since the current density underneath it will be smaller for fixed current amplitude. We plan to design such an electrode so that we can cover 90% of the surface area around the leg. A longer electrode along the direction of the leg will be advantageous since it will produce more or less parallel internal current density distributions within several imaging slices around the middle of the electrodes.

Currently, we are planning our first human imaging exper-

iment. A carefully designed experimental protocol is being examined by an institutional review board. In terms of the conductivity image reconstruction algorithm, we will implement various pre- and post-processing capabilities to enhance the image quality.

REFERENCES

[1] N. Zhang, *Electrical Impedance Tomography based on Current Density Imaging*, Toronto, Canada: MS Thesis, Dept. of Elec. Eng, 1992.

[2] E.J. Woo, S.Y. Lee, and C.W. Mun, "Impedance tomography using internal current density distribution measured by nuclear magnetic resonance", *SPIE*, vol. 2299, pp. 377-385, 1994.

[3] Y.Z. Ider, and O. Birgul, "Use of the magnetic field generated by the internal distribution of injected currents for electrical impedance tomography (MR-EIT)", *Elektrik*, vol. 6, pp. 215-225, 1998.

[4] O. Kwon, E.J. Woo, J.R. Yoon, and J.K. Seo, "Magnetic resonance electrical impedance tomography (MREIT): simulation study of J-substitution algorithm", *IEEE Trans. Biomed. Eng.*, vol. 49, pp. 160-167, 2002.

[5] E.J. Woo, J.K. Seo, and S.Y. Lee, "Magnetic resonance electrical impedance tomography (MREIT) in Holder D ed.", *Electrical Impedance Tomography: Methods, History and Applications*, Bristol, UK: IOP Publishing, 2005.

[6] H.J. Kim, B.I. Lee, Y. Cho, Y.T. Kim, B.T. Kang, H.M. Park, S.Y. Lee, J.K. Seo, and E.J. Woo, "Conductivity imaging of canine brain using a 3 T MREIT system: postmortem experiments", *Physiol. Meas.*, vol. 28, pp. 1341-1353, 2007.

[7] H.J. Kim, T.I. Oh, Y.T. Kim, B.I. Lee, E.J. Woo, J.K. Seo, S.Y. Lee, O. Kwon, C. Park, B.T. Kang, and H.M. Park, "*In vivo* electrical conductivity imaging of a canine brain using a 3T MREIT system", *Physiol. Meas.*, vol. 29, pp. 1145-1155, 2008.

[8] B.I. Lee, S.H. Oh, E.J. Woo, S.Y. Lee, M.H. Cho, O. Kwon, J.K. Seo, J.Y. Lee, and W.S. Baek, "Three-dimensional forward solver and its performance analysis in magnetic resonance electrical impedance tomography (MREIT) using recessed electrodes", *Phys. Med. Biol.*, vol. 48, pp. 1971-1986, 2003.

[9] S.H. Oh, B.I. Lee, E.J. Woo, S.Y. Lee, M.H. Cho, O. Kwon,and J.K. Seo, "Conductivity and current density image reconstruction using harmonic B_z algorithm in magnetic resonance electrical impedance tomography", *Phys. Med. Biol.*, vol. 48, pp. 3101-3116, 2003.

[10] S.H. Oh, B.I. Lee, T.S. Park, S.Y. Lee, E.J. Woo, M.H. Cho, O. Kwon, and J.K. Seo, "Magnetic resonance electrical impedance tomography at 3 Tesla field strength", *Mag. Reson. Med.*, vol. 51, pp. 1292-1296, 2004.

[11] S.H. Oh, B.I. Lee, E.J. Woo, S.Y. Lee, T.S. Kim, O. Kwon, and J.K. Seo, "Electrical conductivity images of biological tissue phantoms in MREIT", *Physiol. Meas.*, vol. 26, S279-288, 2005.

[12] T.I. Oh, W. Koo, K.H. Lee, S.M. Kim, J. Lee, S.W. Kim, J.K. Seo, and E.J. Woo, "Validation of a multi-frequency electrical impedance tomography (mfEIT) system KHU Mark1: impedance spectroscopy and time-difference imaging", *Physiol. Meas.*, vol. 29, pp. 295-307, 2008.

[13] C. Park, B.I. Lee, O. Kwon, and E.J. Woo, "Measurement of induced magnetic flux density using injection current nonlinear encoding (ICNE) in MREIT", *Physiol. Meas.*, vol. 28, pp. 117-127, 2006.

[14] T.I. Oh, Y. Cho, Y.K. Hwang, S.H. Oh, E.J. Woo, and S.Y. Lee, "Improved current source design to measure induced magnetic flux density distributions in MREIT", *J. Biomed. Eng. Res.*, vol. 27, pp. 30-37, 2006.

[15] R. Sadleir, S. Grant, S.U. Zhang, B.I. Lee, H.C. Pyo, S.H. Oh, C. Park, E.J. Woo, S.Y. Lee, O. Kwon, and J.K. Seo, "Noise analysis in MREIT at 3 and 11 Tesla field strength", *Physiol. Meas.*, vol. 26, pp. 875-884, 2005.

[16] J.K. Seo, J.R. Yoon, E.J. Woo, and O. Kwon, "Reconstruction of conductivity and current density images using only one component of magnetic field measurements", *IEEE Trans. Biomed. Eng.*, vol. 50, pp. 1121-1124, 2003.

[17] L.A. Geddes, and L.E. Baker, "The specific resistance of biological material: a compendium of data for the biomedical engineer and physiologist", *Med. Biol. Engng.*, vol. 5, pp. 271-293, 1967.

[18] C. Gabriel, S. Gabriel, and E. Corthout, "The dielectric properties of biological tissues: I. literature survey", *Phys. Med. Biol.*, vol. 41, pp. 2231-2249, 1996a.

[19] S. Gabriel, R.W. Lau, and C. Gabriel, "The dielectric properties of biological tissues: II. measurements in the frequency range 10Hz to 20GHz", *Phys. Med. Biol.*, vol. 41, pp. 2251-2269, 1996b.

[20] S. Grimnes, and O.G. Martinsen, Bioimpedance and *Bioelectricity Basics, London*, UK: Academic Press, 2000.

[21] G.C. Scott, M.L.G. Joy, R.L. Armstrong, and R.M. Henkelman, "Measurement of nonuniform current density by magnetic resonance", *IEEE Trans. Med. Imag.*, vol. 10, pp. 362-374, 1991.

[22] G.C. Scott, M.L.G. Joy, R.L. Armstrong, and R.M. Hankelman, "Sensitivity of magnetic resonance current density imaging", *J. Magn. Reson.*, vol. 97, pp. 235-254, 1992.

[23] S.H. Lee, J.K. Seo, C. Park, B.I. Lee, E.J. Woo, S.Y. Lee, O. Kwon, and J. Hahn, "Conductivity image reconstruction from defective data in MREIT: numerical simulation and animal experiment", *IEEE Trans. Med. Imag.*, vol. 25, pp. 168-176, 2006.